2011 50th IEEE Conference on Decision and Control and
European Control Conference (CDC-ECC)
Orlando, FL, USA, December 12-15, 2011

Epidemic Spread in Human Networks

Faryad Darabi Sahneh and Caterina Scoglio

Abstract— **One of the popular dynamics on complex networks is the epidemic spreading. An epidemic model describes how infections spread throughout a network. Among the compartmental models used to describe epidemics, the Susceptible-Infected-Susceptible (SIS) model has been widely used. In the SIS model, each node can be susceptible, become infected with a given infection rate, and become again susceptible with a given curing rate. In this paper, we add a new compartment to the classic SIS model to account for human response to epidemic spread. In our model, each individual can be infected, susceptible, or alert. Susceptible individuals can become alert with an alerting rate if infected individuals exist in their neighborhood. Due to a newly adopted cautious behavior, an individual in the alert state is less probable to become infected. The problem is modeled as a continuous-time Markov process on a generic graph and then formulated as a set of ordinary differential equations. The model is then studied using results from spectral graph theory and center manifold theorem. We analytically show that our model exhibits two distinct thresholds in the dynamics of epidemic spread. Below the first threshold, infection dies out exponentially. Beyond the second threshold, infection persists in the steady state. Between the two thresholds, infection spreads at the first stage but then dies out asymptotically as the result of increased alertness in the network. Finally, simulations are provided to support our findings.**

I. Introduction

Modeling human reactions to the spread of infectious disease is an important topic in current epidemiology [1], and has recently attracted a substantial attention [2]–[8]. The challenges in this topic concern not only how to model human reactions to the presence of epidemics, but also how these reactions affect the spread of the disease itself. In general, human response to an epidemic spread can be categorized in three main types: (1) Change in the system state. For example, in a vaccination scenario individuals go directly from susceptible state to recovered without going through infected state. (2) Change in system parameters as the result of an adopted cautious behavior. For example, as in [7], individuals might choose to use masks, therefore, have a smaller infection rate parameter. (3) Change in the contact topology. For example, due to the perception of a serious danger, individuals reduce or change their contacts with other people who can potentially be infectious [2].

Epidemic modeling has a rich history. In [9] an epidemic model on a homogenous network was studied. Later on, results for heterogeneous networks were reported in [10]. Pastor-Satorras *et. al.* [11] studied epidemic spreading in scale free networks, showing that in these networks the epidemic threshold vanishes with consequent concerns for the robustness of many real complex systems. Wang *et. al.* [12] provided the first result for a non-synthetic contact topology, and studied the epidemic spread dynamic on a generic graph. Through a local analysis of a mean-field discrete model, it was shown that the epidemic threshold is directly related to the inverse of the spectral radius of the adjacency matrix of the contact graph. More detailed proof was provided in [13]. Ganash *et. al.* [14] proved the same result without any mean-field approximations. A continuous-time epidemic model was studied by Van Mieghem *et. al.* [15], where a set of ordinary differential equations was extracted through mean-field approximation of a continuous time Markov process. The relation between the epidemic threshold and the spectral radius was rigorously proved and further insights about the steady state infection probabilities were analytically derived. Preciado and Jadbabaie [16] studied the epidemic spread on geometric random networks and then investigated [17] the epidemic threshold on graphs with respect to the network structural information.

A good review on the existing results studying the interaction of the epidemic spreading and the human behavior can be found in [2]. Poletti *et. al.* [18] developed a population-based model where susceptible individuals could choose between two behaviors in response to presence of infection. Funk *et. al.* [4] showed that awareness of individuals about the presence of a disease can help reducing the size of the epidemic outbreak. In their paper, awareness and disease have interconnected dynamics. Theodorakopoulos *et. al.* [8] formulated the problem so that individuals could make decision based on the perception of the epidemic size. Perra *et. al.* [19] considered the case where individuals go to a "*feared*" state when they sense infection. Since most of the existing results are for population-based models, they are suitable for a society of well-mixed individuals. To the best of the authors' knowledge, individual-based results have not been reported for this problem so far.

The contribution of this paper is two-fold: (1) Unlike most of the previous results, no homogeneity assumption is made on the contact network and the human-disease interaction in this paper is modeled on a generic contact graph. (2) We show through analytical approaches that two distinct critical values exist for the infection strength. The two are explicitly computed. To the authors' knowledge the existence of two distinct thresholds is reported for the first time in this paper, providing a fundamental progress on previous results.

The rest of the paper is organized as follows. Section II is devoted to the problem formulation and model derivations.

This research was supported by National Agricultural Biosecurity Center at Kansas State University.

Authors are with the Department of Electrical and Computer Engineering, Kansas State University. E-mails: faryad@ksu.edu, caterina@ksu.edu

Stability analysis results of the model are provided in Section III. Finally, results are examined through numerical simulations in Section IV.

II. Model Development

In this section, the N-intertwined SIS model developed in [15] is reviewed briefly. The SAIS spreading model is then introduced as the basis for the future developments in this study.

A. N-Intertwined SIS Model for Epidemic Spread

Van Mieghem *et. al.* [15] derived a set of ordinary differential equations, called the N-intertwined model, which represents the time evolution of the probability of infection for each individual. In this model, a network of N individuals is considered where each individual is represented by a node and the contact topology is represented by a graph $\mathcal{G}$. A disease in this model is characterized by infection rate $\beta \in \mathbb{R}^+$ and curing rate $\delta \in \mathbb{R}^+$. The N-intertwined model describes the time evolution of the infection probability of the i-th individual, denoted by $p_i \in [0,1]$, as

$$\dot{p}_i = \beta(1-p_i)\sum_{j\in\mathcal{N}_i} a_{ij}p_j - \delta p_i,\ i \in \{1,...,N\}, \quad (1)$$

where $a_{ij} > 0$ if individual j can potentially infect individual i, i.e. $j \in \mathcal{N}_i$, otherwise $a_{ij} = 0$.

Proposition 1: Consider the N-intertwined model (1). Initial infection will die out exponentially if the infection strength $\tau \triangleq \frac{\beta}{\delta}$ satisfies

$$\tau \triangleq \frac{\beta}{\delta} \leq \frac{1}{\rho(A)}, \quad (2)$$

where $\rho(A)$ is the spectral radius of the adjacency matrix $A = [a_{ij}] \in \mathbb{R}^{N\times N}$ of the contact graph.

Remark 1: The value $\tau_c \triangleq \frac{1}{\rho(A)}$ is usually referred to as the epidemic threshold. For any infection strength $\tau > \tau_c$, infection will persist in the steady state. The following result discusses the steady state values for infection probabilities.

Proposition 2: If the infection strength is above the epidemic threshold, the steady state values of the infection probabilities, denoted by p_i^{ss} for the i-th individual, is the non-trivial solution of the following set of equations

$$\frac{\beta}{\delta}\sum_{j\in\mathcal{N}_i} a_{ij}p_j^{ss} = \frac{p_i^{ss}}{1-p_i^{ss}},\quad i \in \{1,...,N\}. \quad (3)$$

B. SAIS Spreading Model

In this paper, we have built our modeling based on the N-intertwined model. Specifically, we add a new compartment to the classic SIS model for epidemic spread modeling to propose a Susceptible-Alert-Infected-Susceptible (SAIS) model. The contact topology in this formulation is considered as a generic graph. Each node is allowed to be in one of the three states *"S: susceptible"*, *"I: infected"*, and *"A: alert"*. A susceptible individual becomes infected by the infection rate β times the number of its infected neighbors. An infected individual recovers back to the susceptible state by the curing rate δ. An individual can observe the states of its neighbors. A susceptible individual might go to the alert state if surrounded by infected individuals. Specifically, a susceptible node becomes alert with the alerting rate $\kappa \in \mathbb{R}^+$ times the number of infected neighbors. An alert individual can get infected in a process similar to a susceptible individual but with a smaller infection rate $0 \leq \beta_a < \beta$. We assume that transition from an alert individual to a susceptible state is much slower than other transitions. Hence, in our modeling setup, an alert individual never goes back directly to the susceptible state. The stochastic compartmental transitions of a node with one single infected neighbor are depicted in Fig. 1.

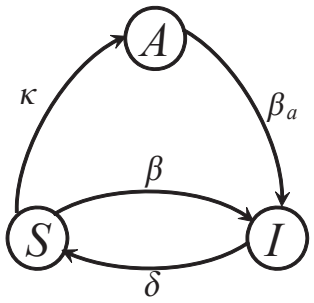

Fig. 1. Stochastic compartmental transition graph for an individual with only one infected neighbor.

For each node $i \in \{1,...,N\}$, define a random variable $X_i : \{S, I, A\} \to \{0, 1, 2\}$. Denote X_i^t the value of X_i at time t for node i. The epidemic spread dynamics is modeled as the following continuous-time Markov process

$$\begin{aligned}
&P(X_i^{t+\Delta t} = 1 | X_i^t = 0, \mathbf{X}^t) = \beta\Delta t Y_i^t + o(\Delta t),\\
&P(X_i^{t+\Delta t} = 0 | X_i^t = 1, \mathbf{X}^t) = \delta\Delta t + o(\Delta t),\\
&P(X_i^{t+\Delta t} = 2 | X_i^t = 0, \mathbf{X}^t) = \kappa\Delta t Y_i^t + o(\Delta t),\\
&P(X_i^{t+\Delta t} = 1 | X_i^t = 2, \mathbf{X}^t) = \beta_a\Delta t Y_i^t + o(\Delta t), \quad (4)
\end{aligned}$$

for $i \in \{1,...,N\}$ and $Y_i^t \triangleq \sum_{j\in\mathcal{N}_i} a_{ij}1_{\{X_j^t=1\}}$. In (4), $P(\cdot)$ denotes probability, $\mathbf{X}^t \triangleq \{X_i^t, i = 1,...,N\}$ is the joint state of the network, $\Delta t > 0$ is a time step, and the indicator function $1_{\{\mathcal{X}\}}$ is one if $\mathcal{X}$ is true and zero otherwise. A function $f(\Delta t)$ is said to be $o(\Delta t)$ if $\lim_{\Delta t\to 0}\frac{f(\Delta t)}{\Delta t} = 0$.

A common approach for studying a continuous-time Markov process is to derive the corresponding Kolmogorov forward (backward) differential equations (see [20]). As can be seen from the above equations, the conditional transition probabilities of a node are expressed in terms of the current state of its neighboring nodes. Therefore, each state of the Kolmogorov differential equations corresponding to the Markov process (4) will be the probability of being in a specific joint state. In this case, we will end up with a set of first order ordinary differential equations of the order 3^N. Hence, the analysis will become dramatically complicated as the network size grows. Using a proper mean-field-like approximation (cf. [15] and [17]), it is possible to express the transition probabilities in terms of infection probabilities

of the neighbors. Specifically, the term $1_{\{X_j^t=1\}}$ is replaced with $E[1_{\{X_j^t=1\}}]$ in (4). Hence, the following new stochastic process is obtained:

$$\begin{aligned}
&P(X_i^{t+\Delta t}=1|X_i^t=0,\mathbf{X}^t)=\beta\Delta t E[Y_i^t]+o(\Delta t),\\
&P(X_i^{t+\Delta t}=0|X_i^t=1,\mathbf{X}^t)=\delta\Delta t+o(\Delta t),\\
&P(X_i^{t+\Delta t}=2|X_i^t=0,\mathbf{X}^t)=\kappa\Delta t E[Y_i^t]+o(\Delta t),\\
&P(X_i^{t+\Delta t}=1|X_i^t=2,\mathbf{X}^t)=\beta_a\Delta t E[Y_i^t]+o(\Delta t). \quad (5)
\end{aligned}$$

Define a new state $x_i \triangleq [s_i, p_i, q_i]^T$, where s_i, p_i, and q_i denote the probabilities of individual i to be susceptible, infected, and alert, respectively. According to (5), the time evolution of x_i can be described by the following differential equations

$$\dot{x}_i = \Theta_i^T x_i,\ i\in\{1,...,N\}, \quad (6)$$

where

$$\Theta_i \triangleq \begin{bmatrix} -\delta & 0 & \delta \\ \beta_a y_i & -\beta_a y_i & 0 \\ \beta y_i & \kappa y_i & -(\beta+\kappa)y_i \end{bmatrix} \quad (7)$$

is the infinitesimal transition matrix and $y_i \triangleq \sum_{j\in\mathcal{N}_i} a_{ij}p_j$. One property of the dynamic system (6) is that $s_i+p_i+q_i$ is a preserved quantity. Hence, the states s_i, p_i, and q_i are not independent. Omitting s_i in (6), the SAIS spreading model is obtained as:

$$\dot{p}_i = \beta(1-p_i-q_i)\sum_{j\in\mathcal{N}_i} a_{ij}p_j + \beta_a q_i \sum_{j\in\mathcal{N}_i} a_{ij}p_j - \delta p_i, \quad (8)$$

$$\dot{q}_i = \kappa(1-p_i-q_i)\sum_{j\in\mathcal{N}_i} a_{ij}p_j - \beta_a q_i \sum_{j\in\mathcal{N}_i} a_{ij}p_j, \quad (9)$$

for $i\in\{1,...,N\}$.

III. Analysis of SAIS Spreading Model

In this section, the SAIS spreading model (8) and (9) derived in the previous section is analyzed.

A. Comparison between SAIS and SIS

In this section, the SAIS model and the SIS model are compared with respect to the infection probabilities of the individuals. Specifically, we are interested to compare $p_i(t)$, the response of (8) and (9), with infection probability $p_i'(t)$ in the N-intertwined SIS model, which is the solution of the system

$$\dot{p}_i' = \beta(1-p_i')\sum_{j\in\mathcal{N}_i} a_{ij}p_j' - \delta p_i'. \quad (10)$$

The following theorem shows that alertness decreases the probability of infection for each individual.

Theorem 1: Starting with the same initial conditions $p_i(t_0) = p_i'(t_0)$, $i=\{1,...,N\}$, the infection probabilities of individuals in SIS model (10) always dominate those of the SAIS model (8) and (9), i.e.,

$$p_i(t) \le p_i'(t), i=\{1,...,N\}\ \ \forall t\in[t_0,\infty). \quad (11)$$

Proof: Rewrite the equation (8) as

$$\dot{p}_i = \beta(1-p_i)\sum_{j\in\mathcal{N}_i} a_{ij}p_j - \delta p_i - (\beta-\beta_a)q_i\sum_{j\in\mathcal{N}_i} a_{ij}p_j. \quad (12)$$

Starting with the same initial conditions $p_i(t_0)=p_i'(t_0)$ for $i\in\{1,...,N\}$, it is concluded that

$$p_i(t_0)=p_i'(t_0) \Rightarrow \dot{p}_i(t_0) \le \dot{p}_i'(t_0), \quad (13)$$

since $(\beta-\beta_a)q_i(t_0)\sum_{j\in\mathcal{N}_i} a_{ij}p_j(t_0)$ is a non-negative term having $\beta_a<\beta$ by definition. According to (13), there exists $t_f > t_0$ so that

$$p_i(t) \le p_i'(t), i\in\{1,...,N\}\ \ \forall t\in[t_0,t_f]. \quad (14)$$

The theorem is proved if we show that inequality (14) holds for every $t_f\in(t_0,\infty)$. Assume that there exists $t_1>t_0$, so that (14) holds for $t_f=t_1$ but it is not true for any $t_f>t_1$. Obviously, at $t=t_1$,

$$\exists i\in\{1,...,N\} \text{ s.t. } p_i(t_1)=p_i'(t_1) \text{ and } \dot{p}_i(t_1) > \dot{p}_i'(t_1). \quad (15)$$

In the subsequent arguments, it is shown that no such t_1 exists. From (12), $\dot{p}_i(t_1)$ is found to satisfy

$$\begin{aligned}
\dot{p}_i(t_1) &= \beta(1-p_i(t_1))\sum_{j\in\mathcal{N}_i} a_{ij}p_j(t_1)\\
&\quad -(\beta-\beta_a)q_i(t_1)\sum_{j\in\mathcal{N}_i} a_{ij}p_j(t_1) - \delta p_i(t_1)\\
&\le \beta(1-p_i(t_1))\sum_{j\in\mathcal{N}_i} a_{ij}p_j(t_1) - \delta p_i(t_1)\\
&= \beta(1-p_i'(t_1))\sum_{j\in\mathcal{N}_i} a_{ij}p_j(t_1) - \delta p_i'(t_1), \quad (16)
\end{aligned}$$

according to (15) and the fact that $(\beta-\beta_a)q_i(t_1)\sum a_{ij}p_j(t_1)$ is a non-negative term. Based on (14), $\forall j\in\{1,...,N\}$ we have $p_j(t_1)\le p_j'(t_1)$. Therefore, the inequality (16) is further simplified as

$$\dot{p}_i(t_1) \le \beta(1-p_i'(t_1))\sum_{j\in\mathcal{N}_i} a_{ij}p_j'(t_1) - \delta p_i'(t_1) = \dot{p}_i'(t_1). \quad (17)$$

Having $\dot{p}_i(t_1)\le\dot{p}_i'(t_1)$ contradicts (15). Hence, no such t_1 exists so that (15) is true. As a result, the inequality (14) holds for every $t_f\in(t_0,\infty)$. This completes the proof. ■

B. Exponential Epidemic Die-Out

Theorem 2: Consider the SAIS spreading model (8) and (9). Assume that the infection strength satisfies

$$\tau = \frac{\beta}{\delta} < \frac{1}{\rho(A)}. \quad (18)$$

Then, initial infections will die out exponentially.

Proof: The solution of $p_i(t)$ was proved in Theorem 1 to be upper-bounded by $p_i'(t)$. According to Proposition 1, the N-intertwined model (10) is exponentially stable if (18) is satisfied. As a consequence, $p_i(t)$ in (12) is also exponentially stable if (18) is satisfied. ■

C. Asymptotically Epidemic Die-Out

According to (9),

$$q_i^e = \frac{1-p_i}{1+\frac{\beta_a}{\kappa}},\ i \in \{1,...,N\}, \tag{19}$$

is an equilibrium for (9). To facilitate the subsequent analysis, define a new state r_i as

$$r_i \triangleq q_i - q_i^e = q_i - \frac{1-p_i}{1+\frac{\beta_a}{\kappa}}. \tag{20}$$

Substituting $q_i = r_i + \frac{1}{1+\frac{\beta_a}{\kappa}} - \frac{p_i}{1+\frac{\beta_a}{\kappa}}$ from (20) in (8) and (9), the derivatives $\dot{p}_i$ and $\dot{r}_i$ in the new coordinate are derived as

$$\begin{aligned}\dot{p}_i = &\{\beta\frac{\frac{\beta_a}{\kappa}}{1+\frac{\beta_a}{\kappa}} + \beta_a\frac{1}{1+\frac{\beta_a}{\kappa}}\}\sum_{j\in\mathcal{N}_i} a_{ij}p_j \\ &- \{\beta + \frac{\beta+\beta_a}{1+\frac{\beta_a}{\kappa}}\}p_i\sum_{j\in\mathcal{N}_i} a_{ij}p_j \\ &- (\beta-\beta_a)r_i\sum_{j\in\mathcal{N}_i} a_{ij}p_j - \delta p_i, \end{aligned}\tag{21}$$

$$\dot{r}_i = -\kappa(1+\frac{\beta_a}{\kappa})r_i\sum_{j\in\mathcal{N}_i} a_{ij}p_j. \tag{22}$$

To facilitate the subsequent analysis, define

$$\mathbf{p} \triangleq [p_1,...,p_N]^T \in \mathbb{R}^N,\ \mathbf{r} \triangleq [r_1,...,r_N]^T \in \mathbb{R}^N. \tag{23}$$

According to (21) and (22) and the definitions (23), the followings are true

$$\dot{\mathbf{p}} = (\beta_{eff}A - \delta I)\mathbf{p} + G_1(\mathbf{p},\mathbf{r}), \tag{24}$$

$$\dot{\mathbf{r}} = \mathbf{0}\mathbf{r} + G_2(\mathbf{p},\mathbf{r}), \tag{25}$$

where $\mathbf{0}$ is a matrix or vector of appropriate dimensions,

$$\beta_{eff} \triangleq \beta\frac{\frac{\beta_a}{\kappa}}{1+\frac{\beta_a}{\kappa}} + \beta_a\frac{1}{1+\frac{\beta_a}{\kappa}}, \tag{26}$$

and

$$G_k(\cdot) \triangleq [g_{k,1}(\cdot),...,g_{k,N}(\cdot)]^T, \tag{27}$$

for $k \in \{1,2\}$ with

$$\begin{aligned} g_{1,i}(\mathbf{p},\mathbf{r}) \triangleq &-\{\beta + \frac{\beta+\beta_a}{1+\frac{\beta_a}{\kappa}}\}p_i\sum_{j\in\mathcal{N}_i} a_{ij}p_j \\ &- (\beta-\beta_a)r_i\sum_{j\in\mathcal{N}_i} a_{ij}p_j, \end{aligned}\tag{28}$$

$$g_{2,i}(\mathbf{p},\mathbf{r}) \triangleq -\kappa(1+\frac{\beta_a}{\kappa})r_i\sum_{j\in\mathcal{N}_i} a_{ij}p_j. \tag{29}$$

If we linearize the system (24) and (25) at the origin, the resulting system has N zero eigenvalues. Therefore, linearization technique fails to investigate the stability properties of (24) and (25). In the following arguments, we show that center manifold theory can be employed here.

The eigenvalues of matrix $(\beta_{eff}A - \delta I)$ are $\beta_{eff}\lambda_i - \delta, i \in \{1,...N\}$, where λ_i's are the eigenvalues of the adjacency matrix A. Therefore, assuming that

$$\frac{\beta_{eff}}{\delta} < \frac{1}{\rho(A)}, \tag{30}$$

the matrix $(\beta_{eff}A - \delta I)$ is Hurwitz (i.e., a matrix that all of its eigenvalues have negative real parts). In addition, the two nonlinear functions G_1 and G_2 defined in (27) satisfy

$$G_k(\mathbf{0},\mathbf{0}) = \mathbf{0},\ \nabla G_k(\mathbf{0},\mathbf{0}) = \mathbf{0}, \tag{31}$$

for $k \in \{1,2\}$, where ∇ is the gradient operator. The center manifold theorem (see [21] for more details) suggests that there exists a function $H(\cdot): \mathbb{R}^N \to \mathbb{R}^N$ where the dynamics (24) and (25) can be determined by

$$\dot{\hat{\mathbf{r}}} = G_2(H(\hat{\mathbf{r}}),\hat{\mathbf{r}}). \tag{32}$$

Differential equation (32) can be written in terms of its entries as

$$\dot{\hat{r}}_i = -\kappa(1+\frac{\beta_a}{\kappa})\hat{r}_i\sum_{j\in\mathcal{N}_i} a_{ij}h_j(\hat{\mathbf{r}}), \tag{33}$$

for $i \in \{1,...,N\}$, where $h_i(\cdot)$ is the i-th component of $H(\cdot) \triangleq [h_1(\cdot),...,h_N(\cdot)]^T$.

Remark 2: Usually, it is not feasible to find $h_i(\cdot)$ explicitly. However, we know that each function $h_i(\cdot)$ is necessarily non-negative since the probability p_i is non-negative.

Lemma 1: The trajectories of (33) will asymptotically converge to the set defined by

$$\Omega = \{\hat{\mathbf{r}} \in \mathbb{R}^N | \hat{r}_i\sum_{j\in\mathcal{N}_i} a_{ij}h_j(\hat{\mathbf{r}}) = 0, i = 1,...,N\}. \tag{34}$$

Proof: Define a continuously differentiable function V as

$$V \triangleq \frac{1}{2}\hat{\mathbf{r}}^T\hat{\mathbf{r}}. \tag{35}$$

Taking the derivative of V with respect to time, we have

$$\dot{V} = \sum_{i=1}^N \hat{r}_i\dot{\hat{r}}_i = -\kappa(1+\frac{\beta_a}{\kappa})\sum_{i=1}^N\left(\hat{r}_i^2\sum_{j\in\mathcal{N}_i} a_{ij}h_j(\hat{\mathbf{r}})\right). \tag{36}$$

It can be seen that the time derivative $\dot{V}$ is negative semi-definite according to Remark 2. According to the LaSalle's invariance theorem (see [21]) the trajectories of (33) will asymptotically converge to the set $\dot{V} \equiv 0$, i.e., Ω in (34). ■

Theorem 3: Consider the SAIS spreading model (8) and (9). Assume that the infection strength satisfies (30) where β_{eff} is defined in (26). Small initial infections die out asymptotically as $t \to \infty$.

Proof: Since the infection strength satisfies (30), the matrix $(\beta_{eff}A - \delta I)$ is Hurwitz. According to the property (31) of $G_1(\mathbf{p},\mathbf{r})$, the system

$$\dot{\mathbf{p}} = (\beta_{eff}A - \delta I)\mathbf{p} + G_1(\mathbf{p},\mathbf{0}),$$

which is system (24) with $\mathbf{r} = \mathbf{0}$, is exponentially stable. In addition, according to Lemma 1, $\hat{r}_i\sum_{j\in\mathcal{N}_i} a_{ij}h_j(\hat{\mathbf{r}}) \to \infty$ as $t \to \infty$. Therefore, the term $r_i\sum a_{ij}p_j$ in (21) can be

considered as a vanishing disturbance for (24). Therefore, $p_i \to 0$ asymptotically as $t \to \infty$. ■

Remark 3: From Theorem 2, the first epidemic threshold is

$$\tau_c^1 = \frac{1}{\rho(A)}, \tag{37}$$

which is equal to the epidemic threshold in the N-intertwined SIS epidemic model. If the infection rate β_a is such that

$$\frac{\beta_a}{\delta} < \frac{1}{\rho(A)}, \tag{38}$$

the ratio $\frac{\beta_{eff}}{\delta}$ can be larger or smaller than $\frac{1}{\rho(A)}$, depending on the value of β. Therefore, if (38) holds, Theorem 3 suggests that there exists another epidemic threshold τ_c^2. Using the definition of β_{eff} in (26), the condition (30) in Theorem 3 can be expressed as

$$\frac{\beta_{eff}}{\delta} = \frac{\beta}{\delta}\frac{\frac{\beta_a}{\kappa}}{1+\frac{\beta_a}{\kappa}} + \frac{\beta_a}{\delta}\frac{1}{1+\frac{\beta_a}{\kappa}} \leq \frac{1}{\rho(A)}, \tag{39}$$

which is equivalent to

$$\frac{\beta}{\delta} \leq \frac{1}{\rho(A)} + \frac{\kappa}{\beta_a}\left(\frac{1}{\rho(A)} - \frac{\beta_a}{\delta}\right). \tag{40}$$

From (40), the second epidemic threshold τ_c^2 is

$$\tau_c^2 = \tau_c^1 + \frac{\kappa}{\beta_a}\left(\frac{1}{\rho(A)} - \frac{\beta_a}{\delta}\right). \tag{41}$$

Notice that, according to (38), $\tau_c^2 > \tau_c^1$.

D. Epidemic Persistence in the Steady State

The steady state is studied by letting the time derivatives $\dot{p}_i$ and $\dot{q}_i$ equal to zero, namely,

$$0 = \beta(1-p_i^{ss}-q_i^{ss})y_i^{ss} + \beta_a q_i^{ss} y_i^{ss} - \delta p_i^{ss}, \tag{42}$$

$$0 = \kappa(1-p_i^{ss}-q_i^{ss})y_i^{ss} - \beta_a q_i^{ss} y_i^{ss}, \tag{43}$$

where $y_i^{ss} \triangleq \sum_{j\in\mathcal{N}_i} a_{ij} p_j^{ss}$.

From (43), it is inferred that

$$q_i^{ss}\sum a_{ij}p_j^{ss} = \frac{1-p_i^{ss}}{1+\frac{\beta_a}{\kappa}}\sum a_{ij}p_j^{ss}. \tag{44}$$

Now, substitute for $q_i^{ss}\sum a_{ij}p_j^{ss}$ terms in (42) using (44) to get

$$\left(\beta\frac{\frac{\beta_a}{\kappa}}{1+\frac{\beta_a}{\kappa}} + \beta_a\frac{1}{1+\frac{\beta_a}{\kappa}}\right)(1-p_i^{ss})\sum a_{ij}p_j^{ss} - \delta p_i^{ss} = 0. \tag{45}$$

Theorem 4: Consider the SAIS spreading model (8) and (9). The steady state values of the infection probability of each individual in the SAIS model is similar to those of the N-intertwined SIS epidemic model (1) with an effective infection rate β_{eff}.

Proof: Based on the definition of β_{eff} in (26), the equation (45) is simplified to

$$\beta_{eff}(1-p_i^{ss})\sum a_{ij}p_j^{ss} - \delta p_i^{ss} = 0,$$

which can be expressed as

$$\frac{\beta_{eff}}{\delta}\sum a_{ij}p_j^{ss} = \frac{p_i^{ss}}{1-p_i^{ss}}. \tag{46}$$

Comparing (46) with (3) from the Proposition 2, it is observed that the steady state values of the infection probabilities in an SAIS epidemic network is equal to those of a SIS epidemic network with effective infection rate β_{eff}. ■

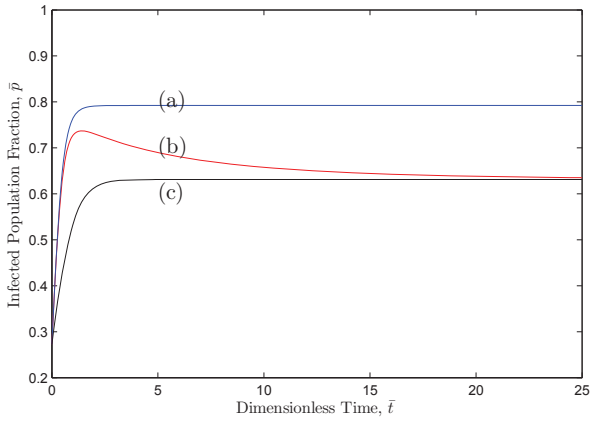

Fig. 2. The infected population fraction in Example 1. (a) SIS model. (b) SAIS model. (c) SIS model with reduced infection rate β_{eff}.

IV. Simulation Results

In order to examine the analytical results developed for the SAIS spreading model, three examples are provided in this section. In all of the simulations, the curing rate is fixed at $\delta = 1$ so that the dimensionless time $\bar{t} = \delta t$ is the same as the simulation time.

Example 1: We consider an arbitrary contact graph with 11 nodes and 16 links. For this network, the spectral radius is found to be $\rho(A) = 3.1385$. For the simulation purpose, three nodes are initialized in the infected state while others are all susceptible. In Fig. 2, three trajectories of the total infection fraction $\bar{p}(t) = \frac{1}{N}\sum_{i=1}^{N} p_i(t)$ are plotted. For all the three, $\kappa = 0.1$ and $\beta_a = 0.1$. The trajectories (a) and (b) correspond to the N-intertwined SIS model 1 and the SAIS spreading model (8) and (9), respectively, with $\beta = 2$. Trajectory (c) is the solution of the SIS model with the infection rate β_{eff} defined in (26).

As is expected from Theorem 1, the infected fraction in SIS model always dominates the SAIS model. In addition, as proved in Theorem 4, the steady state infection fraction in the SAIS is equal to that of the SIS model with the effective infection rate β_{eff}. In Fig. 2, it can be observed that the infection probabilities in the SAIS model spread similar to the SIS model at the first stage. Then, the size of the epidemics is reduced due to increased alertness in the network.

Example 2: In this example, for the same network in the previous example, (1) the steady state value of the infected fraction and (2) the maximum value of the infected fraction are plotted as a function of the infection strength $\tau = \beta/\delta$. The simulation parameters are chosen as $\kappa = 1$, $\beta_a = 0.1$.

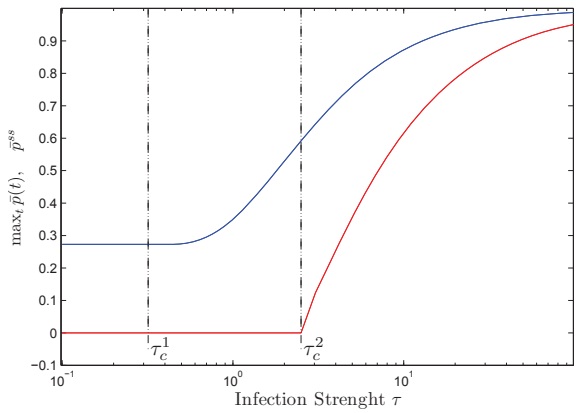

Fig. 3. The maximum infected fraction (blue line) and the steady state value for the infected fraction (red line) in Example 2.

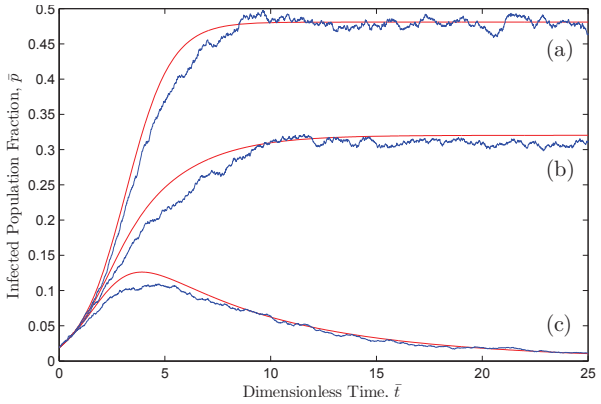

Fig. 4. The infected population fraction in Example 3. (a) SIS model. (b) SAIS model with $\beta_a = 0.02$. (c) SAIS model with $\beta_a = 0.01$.

Since $\beta_a/\delta = 0.1 < 1/\rho(A) = 0.3186$, there exists two distinct thresholds τ_c^1 and τ_c^2 presented in (37) and (41), respectively, as discussed in Remark 3. Simulation results for this example are shown in Fig. 3. As is observed in Fig. 3, the steady state values of the infected fraction $\bar{p}$ is zero before the second epidemic threshold τ_c^2. In addition, the maximum of the infected fraction is equal to the initial infected fraction before τ_c^1, because before τ_c^1, the epidemics dies out exponentially; as stated in Theorem 2. Between the two thresholds, $\max_t \bar{p}(t)$ is greater than $\bar{p}(0)$ but steady state value $\bar{p}^{ss} = 0$. Therefore, in this region the epidemic spreads at the first stage but then completely dies out as a result of increased alertness. After the second threshold, $\bar{p}^{ss} < \max_t \bar{p}(t)$, i.e., alertness reduced the infection size.

Example 3: Consider an epidemic network where the contact graph is an Erdos-Reyni random graph with $N = 320$ nodes and connection probability $p = 0.2$. The initial infected population is $\%2$ of the whole population. The simulation parameters are $\beta = 0.03$, $\kappa = 0.05$. Three trajectories (a), (b), and (c) are presented in Fig. 4 corresponding to $\beta_a = \beta$, $\beta_a = 0.02$, $\beta_a = 0.01$. For the sake of evaluating the model development in Section II, a Monte-Carlo simulation is also provided for each trajectory, shown in Fig. 4 in blue. As can be seen, there is a reasonable agreement between the proposed model (8) and (9) and the Markov process (4). It can be observed that lowering β_a reduces the steady state infection probability. For a sufficiently small value of β_a infection is mitigated totally at the steady state.

V. Acknowledgement

Authors would also like to thank Dr. Fahmida N. Chowdhury for her constructive comments on this manuscript.

References

[1] N. Ferguson, "Capturing human behaviour," *Nature*, vol. 446, no. 7137, p. 733, 2007.

[2] S. Funk, M. Salath, and V. A. A. Jansen, "Modelling the influence of human behaviour on the spread of infectious diseases: a review," *Journal of The Royal Society Interface*, vol. 7, pp. 1247–1256, 2010.

[3] S. Kitchovitch and P. Lio, "Risk perception and disease spread on social networks," *Procedia Computer Science*, vol. 1, no. 1, pp. 2339–2348, 2010.

[4] S. Funk, E. Gilad, C. Watkins, and V. Jansen, "The spread of awareness and its impact on epidemic outbreaks," *Proceedings of the National Academy of Sciences*, vol. 106, no. 16, pp. 6872–6877, 2009.

[5] S. Funk, E. Gilad, and V. Jansen, "Endemic disease, awareness, and local behavioural response," *Journal of Theoretical Biology*, vol. 264, no. 2, pp. 501–509, 2010.

[6] I. Kiss, J. Cassell, M. Recker, and P. Simon, "The impact of information transmission on epidemic outbreaks," *Mathematical biosciences*, vol. 225, no. 1, pp. 1–10, 2010.

[7] S. Tracht, S. Del Valle, J. Hyman, and D. Carter, "Mathematical modeling of the effectiveness of facemasks in reducing the spread of novel influenza a (h1n1)," *PloS ONE*, vol. 5, no. 2, p. e9018, 2010.

[8] G. Theodorakopoulos, J.-Y. L. Boudec, and J. S. Baras, "Selfish response to epidemic propagation," in *American Control Conference*, 2011, to apear.

[9] N. Bailey, *The mathematical theory of infectious diseases and its applications*. London, 1975.

[10] Y. Moreno, R. Pastor-Satorras, and A. Vespignani, "Epidemic outbreaks in complex heterogeneous networks," *The European Physical Journal B - Condensed Matter and Complex Systems*, vol. 26, pp. 521–529, 2002.

[11] R. Pastor-Satorras and A. Vespignani, "Epidemic dynamics and endemic states in complex networks," *Phys. Rev. E*, vol. 63, no. 6, p. 066117, May 2001.

[12] Y. Wang, D. Chakrabarti, C. Wang, and C. Faloutsos, "Epidemic spreading in real networks: An eigenvalue viewpoint," *Proc. 22nd Int. Symp. Reliable Distributed Systems*, pp. 25–34, 2003.

[13] D. Chakrabarti, Y. Wang, C. Wang, J. Leskovec, and C. Faloutsos, "Epidemic thresholds in real networks," *ACM Transactions on Information and System Security*, vol. 10, no. 4, pp. 1–26, 2008.

[14] A. Ganesh, L. Massoulie, and D. Towsley, "The effect of network topology on the spread of epidemics," in *Proceedings IEEE INFOCOM*, vol. 2, 2005, pp. 1455–1466.

[15] P. Van Mieghem, J. Omic, and R. Kooij, "Virus spread in networks," *IEEE/ACM Transactions on Networking*, vol. 17, no. 1, pp. 1–14, 2009.

[16] V. Preciado and A. Jadbabaie, "Spectral analysis of virus spreading in random geometric networks," in *Proc. of the 48th IEEE Conference on Decision and Control*. IEEE, 2010, pp. 4802–4807.

[17] ——, "Moment-based analysis of spreading processes from network structural information," *arXiv:1011.4324*, 2010.

[18] P. Poletti, B. Caprile, M. Ajelli, A. Pugliese, and S. Merler, "Spontaneous behavioural changes in response to epidemics," *Journal of Theoretical Biology*, vol. 260, no. 1, pp. 31–40, 2009.

[19] N. Perra, D. Balcan, B. Gonasalves, and A. Vespignani, "Towards a characterization of behavior-disease models," *PLoS ONE*, vol. 6, no. 8, p. e23084, 08 2011.

[20] P. Van Mieghem, *Performance analysis of communications networks and systems*. Cambridge Univ Press, 2006.

[21] H. Khalil and J. Grizzle, *Nonlinear systems*. Prentice hall Englewood Cliffs, NJ, 2002, vol. 3.